

## Image quality assessment of low-dose protocols in cone beam computed tomography of the anterior maxilla

Randi Lynds Ihlis, DDS,<sup>a,b</sup> Nils Kadesjö, PhD,<sup>c</sup> Georgios Tsilingaridis, DDS, PhD,<sup>d,f</sup>  
Daniel Benchimol, DDS, PhD,<sup>e</sup> and Xie Qi Shi, DDS, MSc, PhD<sup>g,h</sup>

**Objectives.** To evaluate overall image quality and visibility of anatomic structures on low-dose cone beam computed tomography (CBCT) scans and the effect of a noise reduction filter for assessment of the anterior maxilla.

**Methods.** We obtained 48 CBCT volumes on 8 skull-phantoms using 6 protocols: 2 clinical default protocols [standard definition (SD) and high definition (HD)] and 4 low-dose protocols, 2 with a noise reduction filter [ultra-low-dose with high definition (ULDHD) and ultra-low-dose (ULD)] and 2 without [low-dose with high definition (LDHD) and low-dose (LD)]. Overall image quality and visibility of 8 anatomic structures were assessed by 5 observers and statistically analyzed using the Wilcoxon signed rank test. Intra- and interobserver agreement was measured using Cohen's weighted kappa.

**Results.** HD provided higher overall image quality than diagnostically required; LD scored lower than diagnostically acceptable. ULDHD, ULD, and LDHD were acceptable. For anatomic structures, ULDHD and ULD were acceptable. LDHD and LD showed significantly inferior visibility for 1 and 4 structures, respectively. Mean values of intra- and interobserver agreement were 0.395 to 0.547 and 0.350 to 0.370, respectively.

**Conclusions.** ULDHD, ULD, and LDHD may be recommended for assessment of impacted maxillary canines. The noise reduction filter affects image quality positively only at low exposure. (Oral Surg Oral Med Oral Pathol Oral Radiol 2021;000:1–9)

Obtaining two-dimensional (2D) radiographic images is common in dentistry when assessing the location of impacted canines, their relation to surrounding anatomic structures, and possible resorption of neighboring teeth.<sup>1-3</sup> When these images cannot provide enough diagnostic information for further treatment planning, current European guidelines recommend supplementing them with a localized small field of view (FOV) cone beam computed tomography (CBCT) volume.<sup>4-6</sup> The most common reason for obtaining a CBCT of the anterior maxillary region in adolescents is to assess impacted maxillary canines and their surrounding structures.<sup>7,8</sup> A missed diagnosis or

delayed treatment results in 48% of patients developing root resorption of permanent adjacent incisors, which then leads to further and often complicated orthodontic, surgical, and prosthetic treatments.<sup>9-11</sup>

Although the acquisition of three-dimensional (3D) CBCT volumes is rapidly increasing in popularity, the increased radiation-associated risks that CBCT entails warrant attention, especially regarding pediatric patients who have at least a three times greater risk for developing cancer from radiation exposure than adults.<sup>6,12,13</sup> The association between radiation exposure and cancer risk is important, and the significance of this risk is made more problematic when considering that the effects of radiation can appear earlier in the life span of young patients.<sup>14-18</sup> A recent dosimetry study of a 10-year-old anthropomorphic child phantom showed that the estimated dose burden for CBCT is 15 to 140 times higher compared with 2 intraoral radiographs, implying an increased risk of children developing radiation-induced cancer later in life.<sup>19</sup> Another study suggests that, even when the same imaging protocols are used, a 10-year-old receives a 30% higher effective dose from a dental CBCT examination than an adolescent would receive.<sup>20</sup> In response to the need to optimize pediatric dental X-ray examinations, the DIMITRA (Dentomaxillofacial paediatric imaging: an investigation toward low-dose radiation induced risks) research group has expanded upon the previously accepted "as low as reasonably achievable" (ALARA) and "as low as diagnostically acceptable" (ALADA) principles in radiology by recommending the use of exposure doses that are as low as diagnostically acceptable, indication-oriented, and patient-specific

<sup>a</sup>PhD Candidate, Department of Clinical Dentistry, University of Bergen, Bergen, Norway.

<sup>b</sup>Resident in Dento-Maxillofacial Radiology, Folk tandvården Dalarna, Falun, Sweden.

<sup>c</sup>Medical Physicist, Department Head of Radiation Physics, Medical Radiation Physics, Karolinska University Hospital, Stockholm, Sweden.

<sup>d</sup>Associate Professor, Senior Consultant, Department of Dental Medicine, Karolinska Institutet, Stockholm, Sweden.

<sup>e</sup>Senior Consultant, Department of Dental Medicine, Karolinska Institutet, Stockholm, Sweden.

<sup>f</sup>Senior Consultant, Center of Pediatric Oral Health, Stockholm, Sweden.

<sup>g</sup>Professor, Senior Consultant, Department of Clinical Dentistry, University of Bergen, Bergen, Norway.

<sup>h</sup>Professor, Senior Consultant, Faculty of Odontology, Malmö University, Sweden.

Received for publication Jun 18, 2021; returned for revision Sep 29, 2021; accepted for publication Oct 3, 2021.

© 2021 The Author(s). Published by Elsevier Inc. This is an open access article under the CC BY license (<http://creativecommons.org/licenses/by/4.0/>)

2212-4403/\$-see front matter

<https://doi.org/10.1016/j.oooo.2021.10.001>

(ALADAIP).<sup>21-23</sup> The ALADAIP principle addresses the importance of conducting radiographic examinations in terms of maintaining diagnostically acceptable image quality for the individual patient's specific task while at the same time carefully applying imaging protocols with the lowest possible dose needed to maintain necessary image quality.

From a clinical point of view, a protocol can be optimized individually by adjusting the kilovolts (kV), milliampere-seconds (mAs), voxel size ( $\mu\text{m}$ ), and number of frames captured when obtaining a scan and by limiting the FOV so that radiation exposure is confined to the anatomic area that is relevant for the diagnostic task in question. Optimized protocols have been investigated for other diagnostic purposes and are reportedly effective in reducing patient dose.<sup>24-26</sup> A study that examined optimized protocols for assessing the lamina dura found that an ultra-low-dose protocol with HD did not differ statistically from the 4 top-ranking protocols tested, implying that even fine structures usually requiring HD can be visualized with lower dose exposures.<sup>27</sup> Some researchers believe that a high-definition CBCT image is needed for diagnosing impacted canines to identify small but clinically relevant tissue or morphologic changes in the tooth and surrounding structures.<sup>23</sup> Low-dose CBCT protocols have also been suggested.<sup>28,29</sup> However, only 1 study, using 1 phantom for protocol testing, has evaluated the image quality of scanning protocols intended for maxillary canine impaction. Although high-dose protocols produce subjectively appealing images, the cost of extra radiation to the patient is not justified if low-dose images that are diagnostically sufficient could potentially limit exposure dose.<sup>30</sup>

Optimization of exposure, such as by developing low-dose protocols, is an effective strategy to reduce patient dose during radiographic examinations. Still, the dramatically reduced exposure inevitably comes with a reduced signal-to-noise ratio (SNR) in the resultant images.<sup>28</sup> Planmeca Oy offers ultra-low-dose protocols with reduced mAs combined with a lower number of pulsed exposures that introduce a reduced SNR in the resulting image. To compensate for the noise caused by low mAs and fewer projections, a noise reduction filter (the Adaptive Image Noise Optimiser [AINO] filter, Planmeca Oy, Helsinki, Finland) is automatically applied to these ultra-low-dose (ULD) and ultra-low-dose with high definition (ULDHD) protocols.

The aims of the present study were twofold: (1) to compare the subjective evaluation of overall image quality of CBCT scans designed to depict impacted maxillary canines exposed with 6 protocols using combinations of exposure parameters and the AINO noise reduction algorithm, and (2) to compare the visualization of 8 anatomic structures as depicted with the 6 protocols.

## MATERIAL AND METHODS

### Experimental design

Eight dry human skulls, previously used as teaching materials at the Karolinska Institute, Huddinge, Sweden, were employed as test phantoms. Because the origins of the specimens were untraceable, the regional ethics review boards in Stockholm (Dnr: 2007/1288-31/2) and in Bergen (Dnr: 161998) concluded that there were no potentially conflicting ethical aspects in the present study.

The dry skulls were used to construct test phantoms as described in an earlier study by Liljeholm et al.<sup>24</sup> Occlusion for each skull was stabilized using dental impression material, both between the maxillary and mandibular teeth as well as between the temporomandibular joint fossa and the condyle bilaterally. Soft tissue was simulated by placing each skull into a clear close-fitted and water-filled plastic bag. The bag was then placed into a cylindrical container made of 5.0-mm thick acrylic, with a diameter of 20 cm. A 4.0  $\times$  6.0-cm plexiglass cylinder was placed underneath each skull to simulate the atlas vertebra and provide balance for each specimen. Air-filled examination gloves were also used as additional stability for each skull's position during exposure (Figure 1).

### CBCT examination

Six CBCT scans were obtained for each of the 8 skulls using the Planmeca ProMax 3D Mid system. The scanning protocols employed in the project consisted of 4 of the existing protocols suggested by the manufacturer, as follows: a standard definition protocol (SD), which is the clinical default protocol for canine impaction; a high definition protocol (HD) usually used for detecting fine details, such as endodontics-related diagnostic tasks; an ultra-low-dose protocol with high definition (ULDHD); and an ultra-low-dose protocol (ULD). Both the ULDHD and the ULD protocols use Planmeca's AINO noise reduction filter. The HD scans had a voxel size of 150  $\mu\text{m}$ , and protocols without HD had a voxel size of 200  $\mu\text{m}$ . Additionally, we tested a low-dose protocol with high definition (LDHD) and a low-dose protocol (LD). These 2 protocols were self-developed and aimed at producing dose levels equivalent to the ULDHD and ULD protocols, respectively, but without the AINO noise reduction algorithm (Table I). All CBCT exposures had a 4.0  $\times$  5.0-cm FOV obtained with a single 210-degree rotation. Representative axial sections from each of the 6 protocols are illustrated in Figure 2.

### Image evaluation

The 48 volumes were randomly coded using Microsoft Excel Worksheet (Redmond, WA, USA) and organized in Romexis (version 3.8.3.R 2014-12-17, Planmeca).

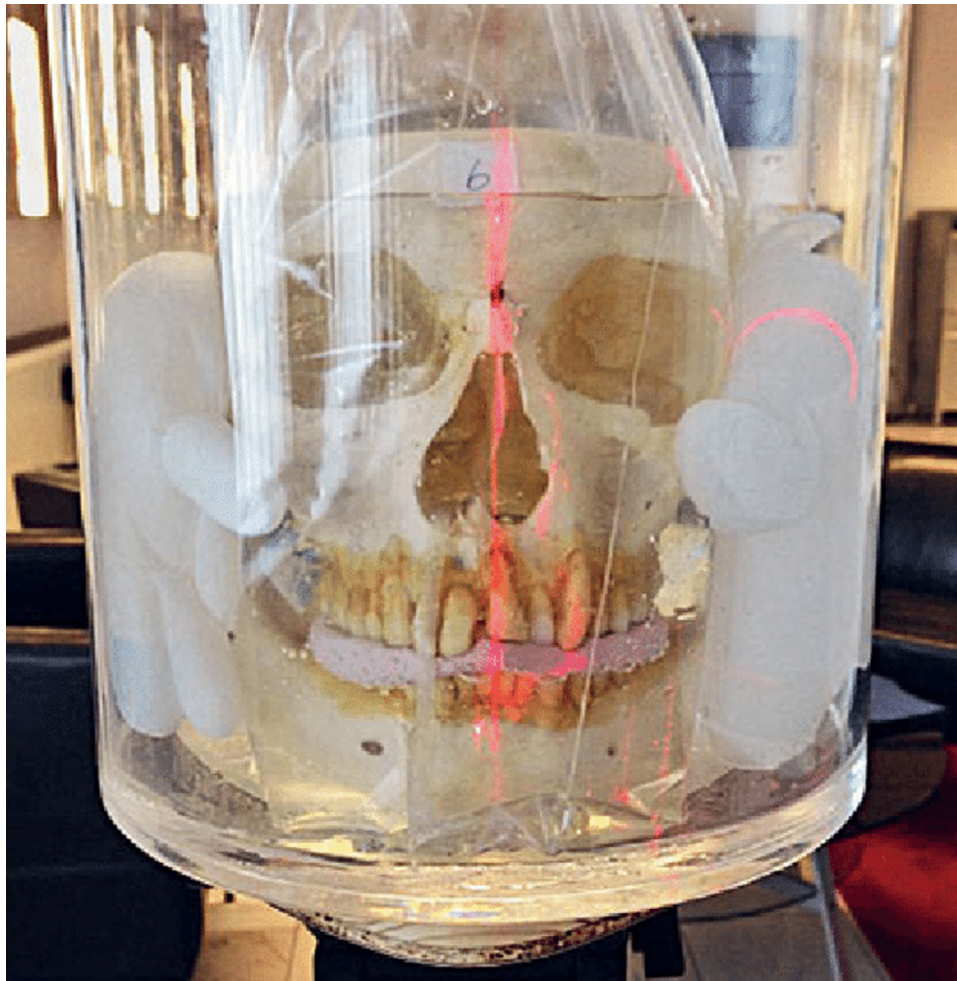


Fig. 1. A skull phantom as prepared for acquisition of the CBCT scans. (Reprinted with permission of the publisher from Lilje-holm et al. 2017.)

**Table I.** Detailed information regarding the exposure protocols

Protocol	Type	Definition	kV	mAs	Voxel size ( $\mu\text{m}$ )	Frames	Nominal DAP ( $\text{mGycm}^2$ )	Dose fraction of the SD (%)
SD*	Standard	Normal	90	96	200	400	329	100%
HD*	Standard	HD	90	150	150	500	514	156%
ULDHD*	ULD	HD	90	36	150	500	122	37%
ULD*	ULD	Normal	90	23	200	400	77	23%
LDHD†	Low-dose	HD	90	38	150	500	129	39%
LD†	Low-dose	Normal	90	22	200	400	74	22%

kV, kilovolts; mAs, milliampere-seconds; DAP, dose area product; SD, standard deviation; HD, high definition; ULD, ultra-low-dose; LD, low-dose.

\*Manufacturer's default protocols: Standard definition (SD): current clinical default for impacted canine examination, High definition (HD), Ultra-low-dose with high definition (ULDHD), Ultra-low-dose (ULD). Both the ULDHD and the ULD protocols use the Planmeca Adaptive Image Noise Optimiser (AINO) noise reduction filter.

†Self-developed protocols. Low-dose with high definition (LDHD) and low-dose (LD) were established to produce dose levels equivalent to the ULDHD and ULD, respectively, but without the quality enhancement AINO algorithm.

Each CBCT data set was assessed independently by 5 specialists in dentomaxillofacial radiology. The observers all had at least 3 years of experience, with a range of 3 to more than 10 years, in the interpretation of CBCT scans. Each observer had prior experience working with Romexis clinically. The observers were

blinded to the exposure protocols and phantom numbers during the image assessments.

All observers examined the images under identical viewing conditions consisting of a dimly lit room and a 19-inch screen with 1280 × 1024 definition (Eizo Flexscan, Model MX190, EIZO Nanao Corporation,

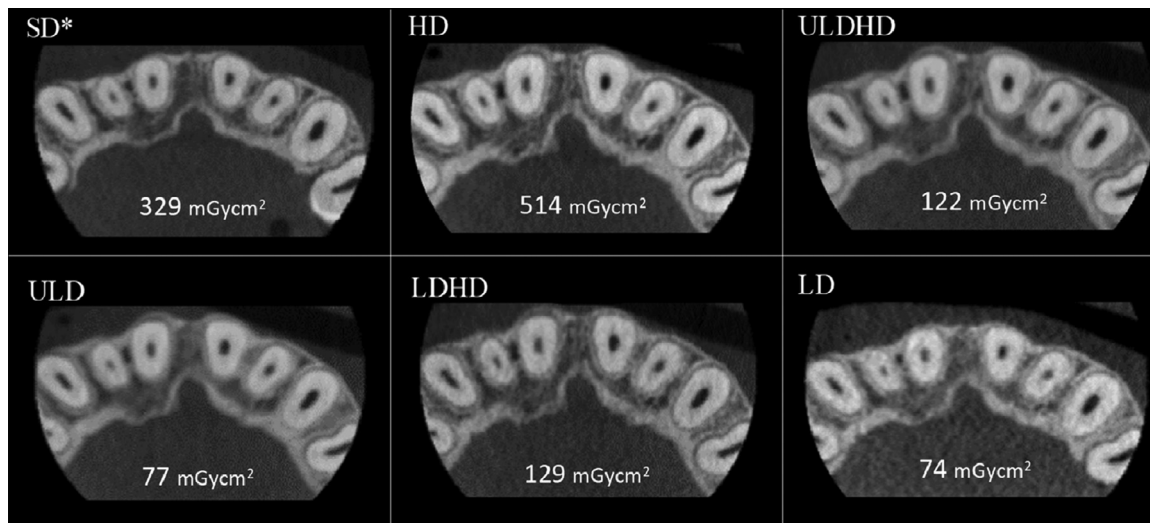


Fig. 2. CBCT axial sections from the same phantom captured using the 6 examination protocols, with the corresponding dose area product (DAP) values. \*SD, standard definition; HD, high definition; UL/DHD, ultra-low-dose with high definition; UL/D, ultra-low-dose; LD/DHD, low-dose with high definition; LD, low-dose. \*Current clinical default setting with standard definition (SD).

Hakui, Ishikawa, Japan). The screen display was adjusted to the Digital Imaging and Communications in Medicine (DICOM) mode enabled by the monitor settings, in which the gray-scale display was calibrated as described by Barten.<sup>31</sup> Image manipulation was allowed, enabling the observers to adjust the grey level, contrast, and multiplanar reconstruction according to their individual preferences.

### Overall image quality and visibility of anatomic structures

The CBCT data sets were evaluated in terms of the overall subjective impression of the quality of the CBCT images of the anterior maxilla and the detectability of anatomic structures. Detailed instructions about the evaluation criteria, including how to rate the overall image quality and the visibility of the structures, were given to all observers.

Image quality was defined as the ability of the image to answer diagnostic questions in the clinical situation of impacted maxillary canines. The overall image quality for each of the 48 CBCT volumes was individually ranked according to an ordinal scale of 1 to 4, in which 1 was poor, 2 was questionable, 3 was good (diagnostically acceptable), and 4 was excellent.

The anatomic structures included a range of radiographically visible landmarks in the anterior maxillary region that commonly provide vital diagnostic information for future orthodontic treatment regarding the interpretation of the canine position as well as possible canine-induced root resorption (Table II). The following structures were assessed: (1) the intermaxillary suture; (2) the incisive foramen and canal(s); (3) the cortical bone of the buccal/palatal surface of the

maxilla; (4) the trabecular bone pattern (spongiosa); (5) the distinction of the grey level difference in enamel, dentin, and pulp; (6) the lamina dura; (7) the periodontal ligament space; and (8) the distinction of the root apex shape. The structures were assessed in terms of their visibility according to an ordinal scale of 1 to 4, in which 1 indicated that the structure was not visible, 2 indicated questionable visibility (diffuse, noisy), 3 indicated that the structure was visible (diagnostically acceptable for the task of assessing impacted maxillary canines), and 4 indicated that the structure was distinctly visible. The most common score value of all observers' answers was considered representative of the overall image quality and the level of visibility for each anatomic structure in question and used for data analysis.

Twelve CBCT scans (from 2 of the 8 skulls) were reassessed by all 5 observers with a time lag of at least 3 weeks. This process provided reproducibility data for 25% of all CBCT images.

### Statistical analyses

The statistical analysis was performed using SPSS (IBM SPSS Statistics, version 27, IBM Corp, Armonk, NY, USA).

The one-sample Wilcoxon signed rank test was applied to determine whether the median of overall image quality and landmark visibility for each of the protocols was significantly different from a hypothetical median, "3," representing the cut-off for diagnostic acceptability according to our ordinal scale. The null hypothesis was that the overall image quality and visibility of each structure were at a diagnostically acceptable level (score 3) for the task of assessing anterior

**Table II.** Anatomic structures examined in the current study and their definitions

Structures	Definition
Intermaxillary suture	Thin radiolucent line interproximal to the central incisors and inferior to the anterior nasal spine, forming the midline of the premaxilla.
Incisive foramen and canal(s)	Ovoid radiolucency in the palate directly posterior to the central incisors (foramen) with radiopaque lateral borders around radiolucencies extending from the anterior floor of the nasal fossae to the anterior maxillary midline (canals).
Cortical bone	Radiopaque borders located on the buccal and palatal surfaces of the alveolar bone.
Trabecular bone pattern (spongiosa)	Cancellous bone located between the cortical plates, visualized as thin radiopaque trabeculae traversing many small radiolucent cavities.
Gray level difference in enamel, dentin, and pulp	Clear distinction between the gray levels of enamel and dentin at the dentinoenamel junction and between dentin and pulp.
Lamina dura	Thin radiopaque line located in the alveolar bone surrounding the roots of the teeth.
Periodontal ligament space	The radiolucent space located between the tooth root and the lamina dura.
Root apex shape	Clear distinction of the shape and contours of the root apices.

maxillary structures, including impacted maxillary canines, for all 6 scanning protocols. The significance level was set at  $P = .05$ .

Intra- and interobserver agreement was established using Cohen's weighted kappa statistics. The outcome was interpreted according to the Landis and Koch scale for observer agreement in assessing categorical data.<sup>32</sup> Kappa scores are interpreted in this scale as almost perfect (0.81-1.0), substantial (0.61-0.80), moderate (0.41-0.60), fair (0.21-0.40), and poor (0.0-0.20).

## RESULTS

Subjective overall image quality differences were seen between some of the examination protocols (Figure 3). The protocols that ranked highest for overall image quality, HD and SD, were the 2 protocols that also had the highest radiation burden for the patient, with HD at 156% of the dose for the reference standard dose (100%), as shown in Table I. The AINO noise reduction filter, applied to the ULDHD and ULD protocols, seemed to be needed only when the exposure was reduced dramatically, such as with the LD protocol.

The overall image quality and visibility of the 8 anatomic structures based on the 5 observers' scores were measured as observed median values for each scanning protocol, using the one-sample Wilcoxon signed rank test (Table III). For the overall image quality, the results of 2 scanning protocols allowed rejection of the null hypothesis; the HD protocol had a significantly higher median value ( $P = .014$ ), and the LD protocol had a significantly lower median value ( $P = .034$ ) than the hypothetical diagnostically acceptable value of "3." The high score for HD required a much larger radiation exposure at 156% of the dose for the SD protocol. The LD protocol required 22% of the SD dose but with a significantly poorer outcome.

With regards to the visibility of anatomic structures, a number of structures had significantly higher medians than "3" (highlighted). Of these, the most

prominent protocol was HD with 6 of the 8 structures receiving significantly higher scores ( $P \leq .020$ ), indicating that the image quality of HD is unnecessarily superior to what is diagnostically needed (Table III). The LDHD protocol had a significantly lower median value than "3" for the precision of identifying the intermaxillary suture ( $P = .020$ ). The LD protocol showed a significantly inferior visibility than the standard in recognizing the intermaxillary suture, trabecular bone pattern, lamina dura, and periodontal ligament space ( $P \leq .017$ ). These findings allow rejection of the null hypothesis regarding visibility of the structures for the LDHD and LD protocols.

Based on all five observers, intraobserver agreement of overall image quality ranged from 0.286 to 0.471 (fair to moderate) with a mean of 0.395, and intraobserver agreement regarding the anatomic structure visibility ranged from 0.485 to 0.66 (moderate to substantial) with a mean of 0.547.<sup>32</sup> Pairwise interobserver agreement based on the 5 observers regarding overall image quality ranged from 0.167 to 0.513 (poor to moderate) with a mean of 0.350, and interobserver agreement regarding anatomic structure visibility ranged from 0.135 to 0.537 (poor to moderate) with a mean of 0.370.<sup>32</sup>

## DISCUSSION

Our results suggest that the overall image quality was at a diagnostically acceptable level for the defined diagnostic task using the following 4 protocols: SD, ULDHD, ULD, and LDHD. HD was rejected due to unnecessarily high image quality, and LD was rejected for producing unacceptably poor image quality.

A compounding problem when trying to determine a radiologist's preference is that a visually pleasing image could subjectively be seen as superior even though an image with lower definition could suffice for accurate interpretation.<sup>33</sup> High-dose exposure protocols with fine spatial definition may be necessary for

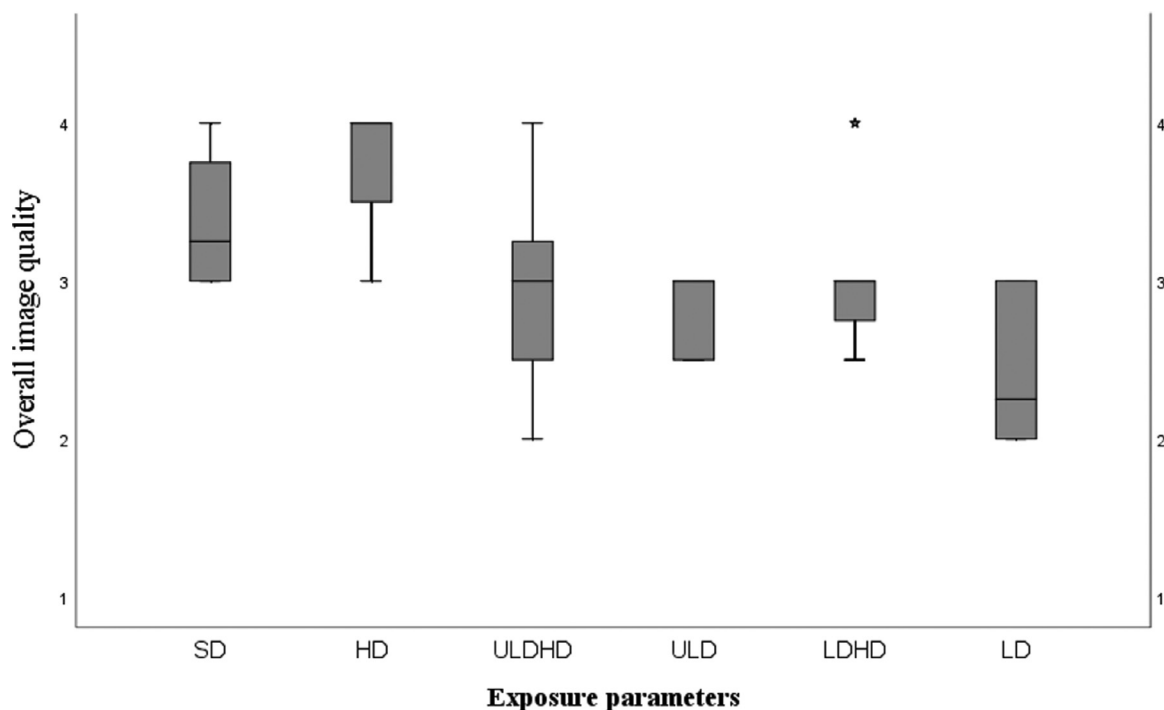


Fig. 3. Overall image quality in relation to exposure protocols. SD, standard definition; HD, high definition; ULDHD, ultra-low-dose with high definition; ULD, ultra-low-dose; LDHD, low-dose with high definition; LD, low-dose. The top of the box represents the 75<sup>th</sup> percentile; the bottom of the box represents the 25<sup>th</sup> percentile, and the middle line represents the median. The whiskers extend from minimum to maximum values, excluding outliers or extreme values. The star beyond the whisker represents an outlier.

**Table III.** One-sample Wilcoxon signed rank test for exposure protocols

	<i>SD median</i> (significance*†)	<i>HD median</i> (significance*†)	<i>ULDHD median</i> (significance*†)	<i>ULD median</i> (significance*†)	<i>LDHD median</i> (significance*†)	<i>LD median</i> (significance*†)
Overall image quality	3.25 (0.063)	4.00 ( <b>0.014</b> )	3.00 (0.783)	3.00 (1.000)	3.00 (0.083)	<u>2.25 (<b>0.034</b>)</u>
Intermaxillary suture	3.00 (0.705)	3.25 (0.098)	2.00 (0.086)	2.00 (0.079)	<u>2.00 (<b>0.020</b>)</u>	<u>2.00 (<b>0.017</b>)</u>
Trabecular bone pattern	3.25 (0.258)	4.00 ( <b>0.019</b> )	3.00 (0.748)	2.00 (0.067)	3.00 (0.102)	<u>2.00 (<b>0.011</b>)</u>
Cortical bone	3.50 ( <b>0.015</b> )	4.00 ( <b>0.007</b> )	3.50 ( <b>0.038</b> )	3.75 (0.052)	3.00 (0.257)	3.00 (0.257)
Incisive foramen and canal(s)	4.00 ( <b>0.005</b> )	4.00 ( <b>0.005</b> )	4.00 ( <b>0.014</b> )	4.00 ( <b>0.025</b> )	3.00 (0.317)	3.00 (0.083)
Gray level difference in enamel, dentin, and pulp	3.50 ( <b>0.046</b> )	4.00 ( <b>0.008</b> )	3.50 ( <b>0.023</b> )	3.50 ( <b>0.034</b> )	3.50 ( <b>0.034</b> )	3.00 (0.157)
Lamina dura	3.00 (1.000)	3.75 (0.052)	3.00 (0.458)	2.75 (0.098)	2.75 (0.129)	<u>2.00 (<b>0.014</b>)</u>
Periodontal ligament	3.25 (0.234)	4.00 ( <b>0.020</b> )	3.25 (0.408)	2.00 (0.058)	2.75 (0.059)	<u>2.00 (<b>0.014</b>)</u>
Root apex shape	4.00 ( <b>0.025</b> )	4.00 ( <b>0.005</b> )	3.25 (0.059)	3.00 (0.180)	3.00 (0.180)	3.00 (0.655)

One-sample Wilcoxon signed rank test for overall image quality and the visibility of the 8 anatomic structures using the hypothetical median of "3" (diagnostically acceptable) for the exposure protocols. The observed medians and their *P* values are listed for each protocol. Data underlined indicates the observed medians that are significantly lower than 3, whereas highlighted data indicates the observed medians that are significantly higher than 3.

*SD*, standard definition; *HD*, high definition; *ULDHD*, ultra-low-dose high definition; *ULD*, ultra-low-dose; *LDHD*, low-dose high definition; *LD*, low-dose.

\*The significance level is  $P = .05$ .

†Asymptotic significance is displayed.

evaluating impacted canines. The HD of these protocols provides a reliable assessment of key anatomic structures in the anterior maxilla, which is paramount for diagnostic and treatment purposes.<sup>23</sup> In the present study, the HD protocol was overqualified when considering that the significantly higher overall quality score came with a greater radiation burden to the patient. Both HD and SD could be replaced by ULDHD, ULD, or LDHD protocols, which all provided diagnostically acceptable image quality for impacted canines while simultaneously reducing the dose for this group of patients by 63%, 77%, and 61%, respectively, compared with the SD protocol. These 3 LD protocols demonstrated the best balance between image quality and radiation burden for diagnosing anatomic structures in the anterior maxilla and are therefore suitable for CBCT examinations for assessing impacted maxillary canines. This finding is in line with a previous study by Rivas et al.,<sup>28</sup> in which a 50% dose reduction could be reached through dose optimization.

Within the scope of the present study, the dose area product (DAP) was used as a feasible way to determine the relative dose reduction between examination protocols. The kV, filtration, and FOV size and position were kept constant. Under these conditions, DAP and effective dose are directly proportional to each other. Thus, a 63% relative difference in DAP corresponded to a 63% relative difference in effective dose. Note that DAP cannot be directly used to compare radiation doses between examinations of different anatomic locations and FOV size or with different X-ray energies (determined by kV and filtration). Different X-ray devices could also have different irradiation geometries, such as the angle of rotation. Comparing DAP under any of those conditions introduces potentially large errors, making effective dose a more valuable tool.<sup>34</sup>

Of the ULDHD, ULD, and LDHD protocols, LDHD stood out as significantly poorer for visualizing the intermaxillary suture ( $P = .020$ ). A plausible reason for this finding is the large variation in the suture among adults. It is difficult to detect when ossification occurs during development, especially when the CBCT voxel size is larger than half of the suture size. The intermaxillary suture has the most delicate details of the anatomic structures that were evaluated, so it was expected to be difficult to visualize. However, impacted canine assessments and their related diagnostic tasks rarely require clear visibility of the intermaxillary suture, and the visibility of this structure may only be indicated in a few select cases.

The median values of structure visibility generally decreased as the radiation dose decreased (Tables I and III). The LD protocol stands out as insufficient because

the observed median values were significantly lower than “3” in detection of the intermaxillary suture, the trabecular bone pattern, the lamina dura, and the periodontal ligament space. Inferior image quality in terms of structure visibility was not observed using the ULD protocol, which had a comparable dose level to the LD protocol (77 mGycm<sup>2</sup> for ULD vs 74 mGycm<sup>2</sup> for LD), indicating the positive effect of the AINO noise reduction filter. Noise within a certain range does not degrade diagnostic performance, as previous studies have shown.<sup>35-37</sup> However, when the exposure is dramatically reduced, the resultant image can have a noisy, distracting visual appearance, and the visibility of subtle anatomic structures may be affected, such as with the LD protocol. In this case, a noise reduction filter might be necessary to compensate for the reduced SNR.

If visualization of fine structures such as the intermaxillary suture, trabecular bone pattern, lamina dura, or periodontal ligament space is not essential for the patient’s clinical situation, the other structures of interest for impacted canines can be seen with the LD protocol.

When deciding on the appropriate method for radiographic analysis in Sweden, the dentomaxillofacial radiologist is responsible for the choice of the applied modality and exposure settings that are deemed necessary for the diagnostic task. Internationally, orthodontists in many instances make this decision. However, there is a lack of scientific evidence illustrating which CBCT dose protocol should be used when examining impacted maxillary canines. To add to the challenge of selecting and optimizing protocols, different clinical situations require patient-specific diagnostic information that is dependent on what the clinician requires for therapeutic planning, even for the same diagnostic task. For example, patients with impacted maxillary canines may require different protocols depending on whether the tooth will be treated with orthodontic force or extracted.<sup>23</sup> When faced with a diagnostic task that requires clearly visible fine details for certain structures, a protocol with a higher exposure and fine spatial definition is needed.

From a clinical point of view, decision making in treating impacted canines can be influenced by information about the position of the canine and the location of canine-induced root resorptions.<sup>5,38</sup> Currently, the management of canine impaction commonly includes acquiring diagnostic information obtained from CBCT, although little is known about how LD protocols could influence the choice of therapy or treatment outcome.<sup>7,8,39</sup> Further clinical studies are needed to identify how the application of LD protocols can be selected and applied, based on information from the present study on the visibility of the anatomic structures.

Intraobserver agreement in this study ranged from fair to substantial. The LD protocols were quite similar to each other, and low intraobserver agreement could be explained by the subtle differences between protocols. Interobserver agreement regarding subjective preference varied greatly between viewers, with weighted kappa values ranging from 0.167 to 0.513, indicating that the radiologists had differing subjective preferences. In the field of radiology, subjective preference in image quality differs depending on the individual who is interpreting the images. To account for this difference, we used the most common score value of the observer's answers to represent the average demand on image quality. Similar levels of agreement can be seen in a previous dose optimization study, although these results are not directly comparable to the current investigation.<sup>24</sup> Our results regarding interobserver agreement reflect the current clinical situation of different subjective preferences on image quality among dentomaxillofacial radiologists. However, observers were given detailed verbal instructions about the evaluation criteria, and no practical calibration was performed using extra CBCT volumes because we used all the skulls that we had available for the study. In the present investigation, most of the observers were not used to viewing LD CBCT images. Therefore, we expect that after more perceptual training and precalibration of observers, the intra- and interobserver agreement may be increased in future studies.

Based on these results, future similar studies on image quality assessment, assuming that a significant difference of 0.5 with a standard deviation of 0.4 is expected using a 4-rank scale, will require a minimum sample size of 8 phantoms. Our measurements resulted in a standard deviation of approximately 0.4. A limitation with our in vitro design was that none of the 8 specimens had canine impaction. The ideal study design would be based on phantoms that are age-appropriate with impacted canines, but such phantoms are difficult to collect. Previous research performed in vivo on patients with impacted canines have evaluated diagnostic accuracy, but to our knowledge none have focused on image quality. Performing this study and applying 6 different protocols in vivo is not ethically practical due to the radiation burden to the patients.

This study tested image quality using dry skull phantoms, and the images for each protocol were standardized in terms of positioning and lack of motion. This precluded a comparison of images with motion artifacts. Our results should be interpreted with caution because, with an in vivo design, we would expect to see artifacts due to the canine overlapping the roots of adjacent teeth, beam hardening/beam starvation effects, motion artifacts, and metal artifacts. Testing and adjusting the proposed ULDHD, ULD, and LDHD

protocols in a clinical situation should be evaluated in future prospective clinical studies.

## CONCLUSIONS

For the CBCT unit Planmeca ProMax 3D Mid, the ULDHD, ULD, and LDHD protocols may be recommended for clinical studies on assessing impacted maxillary canines because these protocols provide comparable diagnostic information with a radiation dose of 23% to 39% of the standard protocol recommended by the manufacturer. Planmeca AINO's noise reduction filter seems to have a positive effect on image quality when the exposure dose is low.

**Funding:** Funding for this study was provided by the Center for Clinical Research, Dalarna, Sweden and Folkhälsan Dalarna, Sweden.

**Presentation:** Preliminary results of this study were presented at the Odontologisk Riksstämman, a national dental conference in Stockholm, Sweden in November 2020 in the form of an oral presentation.

## DECLARATION OF INTEREST

The authors declare that they have no competing interests.

## ACKNOWLEDGMENTS

The authors would like to thank the contributions of all the observers in this study.

## REFERENCES

1. Algerban A, Jacobs R, Lambrechts P, Loozen G, Willems G. Root resorption of the maxillary lateral incisor caused by impacted canine: a literature review. *Clin Oral Investig.* 2009;13:247-255.
2. Botticelli S, Verna C, Cattaneo PM, Heidmann J, Melsen B. Two- versus three-dimensional imaging in subjects with unerupted maxillary canines. *Eur J Orthod.* 2011;33:344-349.
3. Haney E, Gansky SA, Lee JS, et al. Comparative analysis of traditional radiographs and cone-beam computed tomography volumetric images in the diagnosis and treatment planning of maxillary impacted canines. *Am J Orthod Dentofacial Orthop.* 2010;137:590-597.
4. Bjerklin K, Ericson S. How a computerized tomography examination changed the treatment plans of 80 children with retained and ectopically positioned maxillary canines. *Angle Orthod.* 2006;76:43-51.
5. Bjerklin K, Bondemark L. Ectopic maxillary canines and root resorption of adjacent incisors. Does computed tomography (CT) influence decision-making by orthodontists? *Swed Dent J.* 2008;32:179-185.
6. SEDENTEXCT European Commission. Radiation protection no 172. Cone beam CT for dental and maxillofacial radiology (evidence-based guidelines). Available at: <https://ec.europa.eu/energy/sites/ener/files/documents/172.pdf>. Accessed June 18, 2021.
7. Hajem S, Brogårdh-Roth S, Nilsson M, Hellén-Halme K. CBCT of Swedish children and adolescents at an oral and maxillofacial radiology department. A survey of requests and indications. *Acta Odontol Scand.* 2020;78:38-44.

8. Gümürü B, Guldali M, Tarcin B, Idman E, Sertac Peker M. Evaluation of cone beam computed tomography referral profile: retrospective study in a Turkish paediatric subpopulation. *Eur J Paediatr Dent.* 2021;22:66-70.
9. Ericson S, Kuroi PJ. Resorption of incisors after ectopic eruption of maxillary canines: a CT study. *Angle Orthod.* 2000;70:415-423.
10. Zuccati G. Orthodontics and implant therapy to replace a congenitally missing lateral incisor. *J Clin Orthod.* 2004;38:563-567.
11. Barlow ST, Moore MB, Sherriff M, Ireland AJ, Sandy JR. Palatally impacted canines and the modified index of orthodontic treatment need. *Eur J Orthod.* 2009;31:362-366.
12. Marcu M, Hedesiu M, Salmon B, et al. Estimation of the radiation dose for pediatric CBCT indications: a prospective study on ProMax3D. *Int J Paediatr Dent.* 2018;28:300-309.
13. Brenner D, Elliston C, Hall E, Berdon W. Estimated risks of radiation-induced fatal cancer from pediatric CT. *AJR Am J Roentgenol.* 2001;176:289-296.
14. Claus EB, Calvocoressi L, Bondy ML, Schildkraut JM, Wiemels JL, Wrensch M. Dental x-rays and risk of meningioma. *Cancer.* 2012;118:4530-4537.
15. Pearce MS, Salotti JA, Little MP, et al. Radiation exposure from CT scans in childhood and subsequent risk of leukaemia and brain tumours: a retrospective cohort study. *Lancet.* 2012;380:499-505.
16. Bernier MO, Baysson H, Pearce MS, et al. Cohort Profile: the EPI-CT study: a European pooled epidemiological study to quantify the risk of radiation-induced cancer from paediatric CT. *Int J Epidemiol.* 2019;48:379-381g.
17. Memon A, Rogers I, Paudyal P, Sundin J. Dental X-Rays and the risk of thyroid cancer and meningioma: a systematic review and meta-analysis of current epidemiological evidence. *Thyroid.* 2019;29:1572-1593.
18. White SC, Scarfe WC, Schulze RK, et al. The Image Gently in Dentistry campaign: promotion of responsible use of maxillofacial radiology in dentistry for children. *Oral Surg Oral Med Oral Pathol Oral Radiol.* 2014;118:257-261.
19. Kadesjö N, Lynds R, Nilsson M, Shi XQ. Radiation dose from X-ray examinations of impacted canines: cone beam CT vs two-dimensional imaging. *Dentomaxillofac Radiol.* 2018;47:20170305.
20. Theodorakou C, Walker A, Horner K, et al. Estimation of paediatric organ and effective doses from dental cone beam CT using anthropomorphic phantoms. *Br J Radiol.* 2012;85:153-160.
21. Takahashi S. [Publication of ICRP recommendation 26 (author's transl)]. *Radioisotopes.* 1977;26:895-897. [in Japanese].
22. Jaju PP, Jaju SP. Cone-beam computed tomography: time to move from ALARA to ALADA. *Imaging Sci Dent.* 2015;45:263-265.
23. Oenning AC, Jacobs R, Pauwels R, et al. Cone-beam CT in paediatric dentistry: DIMITRA project position statement. *Pediatr Radiol.* 2018;48:308-316.
24. Liljeholm R, Kadesjö N, Benchimol D, Hellén-Halme K, Shi XQ. Cone-beam computed tomography with ultra-low dose protocols for pre-implant radiographic assessment: an in vitro study. *Eur J Oral Implantol.* 2017;10:351-359.
25. Kadesjö N, Benchimol D, Falahat B, Näsström K, Shi XQ. Evaluation of the effective dose of cone beam computed tomography and multi-slice computed tomography for temporomandibular joint examinations at optimized exposure levels. *Dentomaxillofac Radiol.* 2015;44:20150041.
26. Lofthag-Hansen S, Thilander-Klang A, Gröndahl K. Evaluation of subjective image quality in relation to diagnostic task for cone beam computed tomography with different fields of view. *Eur J Radiol.* 2011;80:483-488.
27. EzEldeen M, Stratis A, Coucke W, Codari M, Politis C, Jacobs R. As low dose as sufficient quality: optimization of cone-beam computed tomographic scanning protocol for tooth autotransplantation planning and follow-up in children. *J Endod.* 2017;43:210-217.
28. Hidalgo Rivas JA, Horner K, Thiruvengkatachari B, Davies J, Theodorakou C. Development of a low-dose protocol for cone beam CT examinations of the anterior maxilla in children. *Br J Radiol.* 2015;88:20150559.
29. Oenning AC, Pauwels R, Stratis A, et al. Halve the dose while maintaining image quality in paediatric Cone Beam CT. *Sci Rep.* 2019;9:5521.
30. Ludlow J. Dose and risk in dental diagnostic imaging: with emphasis on dosimetry of CBCT. *Korean J Oral Maxillofac Radiol.* 2009;39.
31. Barten P. *Contrast Sensitivity of the Human Eye and Its Effects on Image Quality.* Bellingham, WA: SPIE Press; 1999:232.
32. Landis JR, Koch GG. The measurement of observer agreement for categorical data. *Biometrics.* 1977;33:159-174.
33. Pauwels R, Seynaeve L, Henriques JC, et al. Optimization of dental CBCT exposures through mAs reduction. *Dentomaxillofac Radiol.* 2015;44:20150108.
34. ICRP. The 2007 recommendations of the International Commission on Radiological Protection. ICRP publication 103. *Ann ICRP.* 2007;37:1-332. <https://pubmed.ncbi.nlm.nih.gov/18082557/>. PMID: 18082557.
35. Näslund EB, Møystad A, Larheim TA, Øgaard B, Kruger M. Cephalometric analysis with digital storage phosphor images: extreme low-exposure images with and without postprocessing noise reduction. *Am J Orthod Dentofacial Orthop.* 2003;124:190-197.
36. Brüllmann D, Witzel V, Willershausen B, d'Hoedt B. Effect of digital noise filters on diagnostic radiographs for the diagnosis of experimental root fractures. *Int J Comput Dent.* 2008;11:107-114.
37. Brüllmann DD, Röhrig B, Sulayman SL, Schulze R. Length of endodontic files measured in digital radiographs with and without noise-suppression filters: an ex-vivo study. *Dentomaxillofac Radiol.* 2011;40:170-176.
38. Christell H, Birch S, Bondemark L, Horner K, Lindh C, consortium SEDENTEXCT. The impact of Cone Beam CT on financial costs and orthodontists' treatment decisions in the management of maxillary canines with eruption disturbance. *Eur J Orthod.* 2018;40:65-73.
39. Izadikhah I, Cao D, Zhao Z, Yan B. Different management approaches in impacted maxillary canines: an overview on current trends and literature. *J Contemp Dent Pract.* 2020;21:326-336.

*Reprint requests:*

Randi Lynds Ihlis, DDS  
 Randi.Lynds@uib.no